Modelling the occurrence and reactivity of hydroxyl radicals in surface waters: implications for the fate of selected pesticides

UNIVERSITÀ DEGLI STUDI DI TORINO

MODELLING THE OCCURRENCE AND REACTIVITY OF HYDROXYL RADICALS IN SURFACE WATERS: IMPLICATIONS FOR THE FATE OF SELECTED PESTICIDES

Davide Vione,[a,*] Radharani Das,[a,b] Francesca Rubertelli,[a] Valter Maurino,[a] Claudio Minero,[a] Stéphane Barbati [c] and Serge Chiron [c]

[a] *Dipartimento di Chimica Analitica, Università degli Studi di Torino, Via Pietro Giuria 5, 10125 Torino, Italy. http://www.chimicadellambiente.unito.it*

[b] *Department of Chemical Engineering, Haldia Institute of Technology, ICARE complex, Haldia 721657, India.*

[c] *Aix-Marseille Universités-CNRS (UMR 6264), Laboratoire de Chimie Provence, Équipe Chimie de L'Environnement Continental – 3, Place Victor Hugo (case 29), 13331 Marseille cedex 3, France.*

* Corresponding author. Tel. +39-011-6707874; Fax +39-011-6707615; E-mail: *davide.vione@unito.it*
URL: *http://naturali.campusnet.unito.it/cgi.bin/docenti.pl/Show?_id=vione*

Abstract

This paper reports a simple model to describe the formation and reactivity of hydroxyl radicals in the whole column of surface freshwater systems. The model is based on empirical irradiation data and it is a function of the water chemical composition (the photochemically significant parameters Non-Purgeable Organic Carbon –NPOC–, nitrate, nitrite, carbonate and bicarbonate), the water body conformation best expressed as the average depth, and the water absorption spectrum in a simplified Lambert-Beer approach. The purpose is to derive the lifetime of dissolved molecules, due to the reaction with $^{\bullet}$OH, on the basis of their second-order rate constants with the hydroxyl radical. It is also proposed a simplified (and approximated) approach to simulate the absorption spectrum of water when the latter is not available, based on the value of the NPOC. Such a simulation can be useful when the model is adopted to describe a degradation scenario for a certain compound, without a direct link to a definite ecosystem. The model was applied to the lifetime of various pesticides in surface water bodies, and it suggested that the lifetime of a given compound can be very variable in different systems, even more than the lifetime of different compounds in the same water body. The variations of the chemical composition and of the depth of the water column are the main reasons for the reported finding.

Keywords: photochemistry; photochemical fate; sensitised photolysis; pollutant photodegradation.

1. Introduction

The persistence in surface waters of dissolved organic compounds, both natural organic molecules and man-made xenobiotics, depends among other factors on their transformation kinetics due to abiotic and biological processes. Transformation by micro-organisms can be very important for readily biodegradable molecules, including most notably the nutrients. Indeed, the latter are often found at low concentration in the dissolved phase of surface waters due to very fast biological degradation [1].

Many organic pollutants such as some pesticides, polycyclic aromatic hydrocarbons, pharmaceuticals and their transformation intermediates are refractory to biological degradation. In such cases the abiotic transformation processes can represent major removal pathways from surface waters. Abiotic transformation includes hydrolysis, oxidation mediated by dissolved species or by metal oxides, such as Fe(III) and Mn(III,IV) (hydro)oxides, and light-induced reactions [2,3].

Photochemical reactions play a very important role among the abiotic transformation processes [4,5]. They involve the direct photolysis of sunlight-absorbing molecules and the indirect phototransformation sensitised by dissolved organic matter and by photoactive compounds such as nitrate, nitrite, and Fe(III) [6-9]. These processes yield reactive species such as the radicals $^{\bullet}OH$ and $CO_3^{-\bullet}$, singlet oxygen ($^1O_2$), and the excited triplet states of Dissolved Organic Matter ($^3DOM^*$). They are all involved into transformation reactions, at a variable extent depending on the chemical composition of surface waters and on the reactivity of the molecules that are being transformed [10-13].

The radical $^{\bullet}OH$ is the most powerful oxidant in surface waters. It is mainly produced by the photolysis of nitrate and nitrite [14] and by the irradiation of DOM [15]. The exact pathway of $^{\bullet}OH$ photoproduction by DOM is still poorly known. It could involve water oxidation by $^3DOM^*$, or photo-Fenton reactions initiated by the photolysis of the complexes between Fe(III) and DOM [16].

$$NO_3^- + h\nu + H^+ \rightarrow {}^{\bullet}OH + {}^{\bullet}NO_2 \quad (1)$$

$$NO_2^- + h\nu + H^+ \rightarrow {}^{\bullet}OH + {}^{\bullet}NO \quad (2)$$

$$DOM + h\nu \rightarrow {}^3DOM^* \quad (3)$$

$$^3DOM^* + H_2O \rightarrow DOM\text{-}H^{\bullet} + {}^{\bullet}OH \quad (4)$$

$$Fe^{III}\text{-}DOM + h\nu + H_2O \rightarrow Fe^{2+} + DOM\text{-}OH^{\bullet} + H^+ \quad (5)$$

$$Fe^{2+} + H_2O_2 \rightarrow FeOH^{2+} + {}^{\bullet}OH \quad (6)$$

The quantification of $^{\bullet}OH$ photogeneration by DOM is by far the most difficult task because DOM is not a species of definite chemical composition: it rather varies in different water bodies. However, in various surface water samples it has recently been possible to find a correlation between the generation rate of $^{\bullet}OH$, unaccounted for by nitrate and nitrite, and the amount of DOM, quantified as Non-Purgeable Organic Carbon (NPOC) [17].

This paper reports on the modelling of the occurrence and reactivity of $^{\bullet}OH$ as a function of the chemical composition and the depth of surface waters. It is based on the calculation of the flow of absorbed photons and of photogenerated hydroxyl radicals within a whole water column, and was applied to the assessment of the lifetime, due to reaction with $^{\bullet}OH$, of different pesticides chosen to ensure a variety of reaction rate constants with the hydroxyl radical. The results of the model were also compared with field data obtained in the surface layer (1 m depth) of Lake Greinfensee, Switzerland [10].

2. Modelling the generation and reactivity of $^{\bullet}OH$ in surface waters

2.1. Modelling the absorption spectrum of surface water

A major issue in the context of surface-water photochemistry is represented by the absorption spectrum of water, which influences the intensity of radiation absorption of the different photoactive species. Indeed all the photosensitisers compete with one another for radiation absorption, with different results that depend on the features of the water body, such as chemical composition and average depth. As a consequence, the absorption spectrum of water is a necessary input datum for a model that describes photochemistry. Such a spectrum is usually expressed as the water absorbance over an optical path length of 1 cm (hereafter $A_1(\lambda)$, the units of which are cm^{-1}). The most significant spectrum is that of water taken from the surface layer: it is the most illuminated compartment and therefore the one where the highest intensity of radiation absorption and the highest rate of the photochemical reactions are observed.

The use of the spectrum of water sampled from the relevant water body is certainly recommended as input datum for the model. However, in some cases it would be interesting to foresee the possible photochemical fate of a pollutant independently of the particular water body, with the purpose of assessing the general degree of photolability of the compound as a function of the ecosystem variables (e.g. chemical composition of water and water column depth). Under these circumstances the variables need not to be linked to a particular case, but should only represent a plausible set of values for actual ecosystems. This *a priori* approach can work if it is possible to simulate the water spectrum from the chemical composition, even with an unavoidable loss of accuracy. In contrast the measurement of the spectrum of a surface water sample would only allow an *a posteriori* approach, in which one has to decide first which water body to consider, obtain water composition data and the absorption spectrum, and finally apply the model to the particular system. In such a case the results will be more accurate, but it would not be possible to break the link between the model and the particular water body under consideration.

This section will be dedicated to the modelling of $A_1(\lambda)$, based on the water chemical composition. Considering that most of the absorption of sunlight in surface waters is carried out by DOM [19], the most significant parameter upon which the spectrum should be based is the Non-Purgeable Organic Carbon (NPOC). The NPOC is the most suitable way to measure the amount of

DOM in waters rich of carbonate and bicarbonate, which would interfere with the measurement of Total Organic Carbon (TOC). In the case of NPOC the water sample is acidified, and the inorganic carbon eliminated as gas-phase CO_2 by purging with a gentle flow of CO_2-free air. It follows the measurement of total carbon [20]. Some volatile organic compounds can be lost in this procedure: on average in lake water it is TOC ≈ 1.3 NPOC [21].

The approach based on NPOC is justified by the fact that there is a good correlation between the water absorbance in the UV (254 and 285 nm) and the NPOC value of surface waters [22,23]. Additionally, the absorption spectra of DOM (and of surface waters as a consequence) follow an exponential-like trend with wavelength [24,25]. These considerations prompt for the fitting of the experimental absorption spectra with a general empirical equation of the form:

$$\frac{A_1(\lambda)}{NPOC} = B \cdot e^{-k \cdot \lambda} \qquad (7)$$

Figure 1 reports the absorption spectra ($A_1(\lambda)$ $NPOC^{-1}$ vs. λ) of different samples taken from the surface layer of freshwater lakes (n = 9, [17,21,26]). The fitting of each spectrum with equation (7) yields different values of B and k. On average one finds that B = 0.45±0.04 L (mg C)$^{-1}$ cm^{-1}, and k = 0.015±0.002 nm^{-1} ($\mu \pm \sigma$). Note that the units of $A_1(\lambda)$ are [cm^{-1}]. Interestingly the value of k is comparable to that reported by Blough and Del Vecchio [25], referred to coastal seawater DOM.

Figure 1 also reports equation (8) (obtained from eq. 7 by substituting the fitting values of B and k) with its error bounds (bold curves), superposed to the experimental absorption spectra. The use of equation (8) enables the modelling of the absorption spectrum of water when the latter is not available. In this way the spectrum $A_1(\lambda)$ might be obtained approximately from the value of NPOC.

$$A_1(\lambda) / NPOC = (0.45 \pm 0.04) \cdot e^{-(0.015 \pm 0.002)\lambda} \qquad (8)$$

2.2. Mass vs. concentration approach in photochemistry models

It was previously indicated that DOM, nitrate and nitrite are the main species involved in the photoinduced production of $^{\bullet}OH$ in surface waters. The assessment of their role in surface-water photochemistry requires the calculation of the intensity of radiation absorption by each compound in the whole column of the aquatic systems.

A problem is represented by the fact that the intensity of sunlight decreases with depth, and its spectrum is also modified [10]. It would therefore be necessary to consider the absorption of the dissolved compounds over the whole water column [27,28]. Also the knowledge of the concentration profile of the species along the whole column of the water body would be required. However, most of the photochemical activity would actually take place in the surface layer (up to

around 1 m depth) [5,29], which is usually thoroughly mixed and has therefore constant chemical composition [30].

For the reasons reported above it might be convenient to adopt a different, approximated but much simpler approach. It is based on the calculation of the intensity of radiation absorption and of the rate of production of the reactive species in the whole volume V = S d. Here d is the water column depth (best expressed as the average depth of the water body), and S is a standard surface area. We have assumed S = 12.6 cm^2 to allow a direct comparison with the results of irradiation experiments of surface water samples [17]. Both the photon flux absorbed by the compound i, P_a^i, and the rate of production of the transient species j, R_j, should therefore be expressed within the volume V. This means that P_a^i will be in units of einstein s^{-1} (1 einstein = 1 mole of photons) and R_j in mol s^{-1}, instead of the more common units of einstein L^{-1} s^{-1} and mol L^{-1} s^{-1}. The actual value of P_a^i will depend on the concentration of i, and in this case it will be used the concentration found in the surface water layer. The reason behind this choice is that the majority of the photochemical reactivity is concentrated in the surface layer where most of the absorption of radiation takes place [10,18]. The model results will be best applicable to the mixing layer of the water bodies. In the case of large, stratified lakes, the water column depth d should be the average depth of the mixing layer.

To achieve the goal of relating all the important quantities to the volume V = S d, consider that the sunlight radiation density reaching the ground ($q°(\lambda)$) is usually expressed in units of einstein cm^{-2} s^{-1} nm^{-1} [31]. For the present purposes it will be sufficient to multiply such a value for the standard surface area S = 12.6 cm^2. The integration over wavelength of $p°(\lambda) = S\ q°(\lambda)$ will give units of einstein s^{-1} as required.

2.3. Radiation absorption by photoactive water components

A major issue into the calculation of the intensity of radiation absorption by a molecule Q in a mixture is that the absorbance A_Q is the same (at equal concentration of Q) in the mixture and when Q is alone in solution. In contrast the absorbed photon flux density p_a^Q and the related fraction of radiation absorption (f_Q) are lower in the mixture, because of competition for absorption between Q and other species. Moreover for two species Q and R at the wavelength λ, the ratio of the absorbance values is equal to the ratio of the absorbed photon flux densities [32]: $A_Q(\lambda)\ A_R(\lambda)^{-1} = p_a^Q(\lambda)\ [p_a^R(\lambda)]^{-1}$. DOM, nitrite and nitrate are the main photochemical sources of $^\bullet OH$ in surface waters [16,17]. For a water column depth d (expressed in cm) at the wavelength λ, the absorbance of nitrate, nitrite and DOM and the total absorbance of the water column (A_{tot}) can be expressed as follows (note that DOM is usually the main radiation absorber above 300 nm [19]):

$$A_{tot}(\lambda) = A_1(\lambda)\ d \quad (9)$$

$$A_{NO3^-}(\lambda) = \varepsilon_{NO3^-}(\lambda)\ d\ [NO_3^-] \quad (10)$$

$$A_{NO2^-}(\lambda) = \varepsilon_{NO2^-}(\lambda)\ d\ [NO_2^-] \quad (11)$$

$$A_{CDOM}(\lambda) = A_{tot}(\lambda) - A_{NO3-}(\lambda) - A_{NO2-}(\lambda) \cong A_{tot}(\lambda) \qquad (12)$$

$A_1(\lambda)$ is the absorbance of water over an optical path length of 1 cm, and ε represents a molar absorption coefficient. Note that $A_1(\lambda)$ could be the actually measured absorption spectrum of water, or could be obtained from the value of NPOC (equation 8). Be $p°(\lambda)$ the incident photon flux density of sunlight (in einstein s^{-1} nm^{-1} over the surface S = 12.6 cm^2). In the Lambert-Beer approximation the total photon flux density absorbed by water is:

$$p_a^{tot}(\lambda) = p°(\lambda) \cdot \left(1 - 10^{-A_{tot}(\lambda)}\right) \qquad (13)$$

For the photon flux density absorbed by DOM, nitrate and nitrite at the wavelength λ, one has to consider that the photon flux densities are proportional to the values of the absorbance [32]:

$$p_a^{DOM}(\lambda) = p_a^{tot}(\lambda)\, A_{DOM}(\lambda)\, [A_{tot}(\lambda)]^{-1} \cong p_a^{tot}(\lambda) \qquad (14)$$

$$p_a^{NO3-}(\lambda) = p_a^{tot}(\lambda)\, A_{NO3-}(\lambda)\, [A_{tot}(\lambda)]^{-1} \qquad (15)$$

$$p_a^{NO2-}(\lambda) = p_a^{tot}(\lambda)\, A_{NO2-}(\lambda)\, [A_{tot}(\lambda)]^{-1} \qquad (16)$$

Finally the total photon flux absorbed by the species i (P_a^i, with i = DOM, NO_3^-, NO_2^-), expressed in einstein s^{-1}, is the integral over wavelength of $p_a^i(\lambda)$.

$$P_a^i = \int_\lambda p_a^i(\lambda)\, d\lambda \qquad (17)$$

Figure 2 reports the absorption spectra $A_1(\lambda)$ of different surface water samples, and in particular four lakes (Avigliana Grande, Avigliana Piccolo, Candia, Rouen, all located in NW Italy) and one lagoon (Rhône river delta, S France) [5,17,21,26]. It also reports the sunlight spectrum adopted for the calculations ($p°(\lambda)$, with 22 W m^{-2} irradiance in the UV, [31]), which corresponds to summertime irradiation conditions. Table 1 reports the values of P_a^{DOM}, P_a^{NO3-} and P_a^{NO2-} for the cited water samples, based on the absorption spectrum, the chemical composition of the surface layer, and the water column depth d [5,17,21,26], for a sunlight UV irradiance of 22 W m^{-2} (see Figure 2). Equation (17) for nitrate, nitrite and DOM was calculated by numerical integration.

2.4. Generation and reactivity of •OH upon irradiation of DOM, nitrate and nitrite

The generation of •OH by the relevant photosensitisers in surface waters is initiated by the absorption of radiation. It is therefore reasonable that the generation rate of •OH by the compound i, $R_{\bullet OH}^i$, is proportional to P_a^i.

The previous paragraph showed how to calculate the absorbed photon fluxes of DOM, nitrate and nitrite from $A_1(\lambda)$, $[NO_3^-]$, $[NO_2^-]$ and d, for a given sunlight irradiance. It is then necessary to

derive the relationships of $R_{\bullet OH}^{DOM}$, $R_{\bullet OH}^{NO3-}$, and $R_{\bullet OH}^{NO2-}$ with the corresponding absorbed photon fluxes. Figure 3 reports the trend of $R_{\bullet OH}$ vs. P_a for nitrate and nitrite under simulated sunlight, based on previously published data [26]. The formation rate of $^{\bullet}OH$ has been measured with the reaction Benzene + $^{\bullet}OH \rightarrow$ Phenol (95% yield, [33]). Irradiation took place under a solar simulator (22 W m^{-2} UV irradiance), inside cylindrical Pyrex cells with surface area S = 12.6 cm^2 [26]. This explains the adoption of S = 12.6 cm^2 as standard in our model. Note that P_a is expressed in einstein s^{-1} and $R_{\bullet OH}$ in mol s^{-1}. The calculation of P_a for nitrate and nitrite was based on the already reported equations (9-17), adopting as $p°(\lambda)$ the emission spectrum of the used lamp (which simulates summertime sunlight).

The derivation of $R_{\bullet OH}^{DOM}$ vs. P_a^{DOM} is more complicated because DOM is not a species of definite chemical composition. Nevertheless, for various surface water samples it has been possible to find a statistically significant correlation between the value of NPOC (that measures DOM) and the formation rate of $^{\bullet}OH$ unaccounted for by nitrate and nitrite ($R_{\bullet OH}^{tot} - R_{\bullet OH}^{NO3-} - R_{\bullet OH}^{NO2-}$) [17]. Such a quantity would measure the generation rate of $^{\bullet}OH$ by DOM, $R_{\bullet OH}^{DOM}$. The correlation that has been found also suggests that the production of $^{\bullet}OH$ by DOM, nitrate and nitrite are independent phenomena, apart from the competition for radiation absorption that is taken into account into the calculation of P_a^i.

Figure 4 reports $R_{\bullet OH}^{DOM} = R_{\bullet OH}^{tot} - R_{\bullet OH}^{NO3-} - R_{\bullet OH}^{NO2-}$ as a function of P_a^{DOM}, calculated as for the previous paragraph (equations 9-17). From linear least-square fitting of the data reported in Figures 3 and 4 one gets the following expressions for the generation rates of $^{\bullet}OH$ from DOM, nitrate and nitrite:

$$R_{\bullet OH}^{DOM} = (3.0 \pm 0.4) \cdot 10^{-5} \; P_a^{DOM} \qquad (18)$$

$$R_{\bullet OH}^{NO3-} = (4.33 \pm 0.17) \cdot 10^{-2} \; P_a^{NO3-} \qquad (19)$$

$$R_{\bullet OH}^{NO2-} = (1.16 \pm 0.03) \cdot 10^{-1} \; P_a^{NO2-} \qquad (20)$$

$$R_{\bullet OH}^{tot} = R_{\bullet OH}^{DOM} + R_{\bullet OH}^{NO3-} + R_{\bullet OH}^{NO2-} \qquad (21)$$

The error bounds represent one standard deviation ($\pm\sigma$). Table 1 reports $R_{\bullet OH}$ for the different surface water samples, calculated on the basis of the corresponding values of P_a with equations (18-21). Note that P_a was determined assuming a sunlight spectrum $p°(\lambda)$ characterised by 22 W m^{-2} UV irradiance (see Figure 2), thus the values of $R_{\bullet OH}$ are referred to the same irradiance.

Once generated, the $^{\bullet}OH$ radicals react quickly with many dissolved compounds. A steady state is promptly reached, where the rate of consumption of $^{\bullet}OH$ is equal to its rate of production. Be S_i a generic scavenger molecule and k_{Si} its second-order rate constant for the reaction with $^{\bullet}OH$. At the steady state the following relationship holds:

$$R_{\bullet OH}^{tot} = \sum_i k_{Si} [^{\bullet}OH] [S_i] = [^{\bullet}OH] \sum_i k_{Si} [S_i] \qquad (22)$$

The main scavengers of hydroxyl radicals in surface freshwaters are DOM, HCO_3^-, CO_3^{2-}, and NO_2^- [10]. From the literature rate constants for reaction with $^\bullet$OH [34], and empirically derived relationships in the case of DOM [17,35], it is possible to express the scavenging rate constant for $^\bullet$OH in freshwater as follows:

$$\sum_i k_{Si} [S_i] = 5\times10^4 \text{ NPOC} + 8.5\times10^6 [HCO_3^-] + 3.9\times10^8 [CO_3^{2-}] + 1.0\times10^{10} [NO_2^-] \qquad (23)$$

Here NPOC is expressed in mg C L^{-1}, and the concentration values are in molarity. $\sum_i k_{Si} [S_i]$ has units of [s^{-1}]. Consider a generic pollutant molecule P, with second-order reaction rate constant $k_{P,\bullet OH}$ with $^\bullet$OH. In the very vast majority of the environmental cases it will be $k_{P,\bullet OH} [P] \ll \sum_i k_{Si} [S_i]$. The rate of P degradation for reaction with $^\bullet$OH ($R_P^{\bullet OH}$) is given by the fraction of $R_{\bullet OH}^{tot}$ that is involved in the degradation of P, namely:

$$R_P^{\bullet OH} = R_{\bullet OH}^{tot} \cdot \frac{k_{P,\bullet OH} \cdot [P]}{\sum_i k_{Si} \cdot [S_i]} \qquad (24)$$

Equation (24) describes a first-order decay kinetics, with rate constant $k_P = R_P^{\bullet OH} V^{-1} [P]^{-1} = R_{\bullet OH}^{tot} k_{P,\bullet OH} (V \sum_i k_{Si} [S_i])^{-1}$. V = S d is the volume of solution contained in a cylinder of surface S = 12.6 cm^2 and height d, which is the average depth of the water body. Note that if [P] is expressed in molarity, V in litres, and $R_P^{\bullet OH}$ in mol s^{-1}, the units of k_P will be [s^{-1}]. The volume V has to be included in the expression of k_P, to obtain compatibility between the mass approach (adopted to simplify the absorbed light calculations) and the kinetic treatment of the results.

For a first-order kinetics it is possible to calculate the half-life time of P, $(t_P^{\bullet OH})_{½} = \ln 2 \, (k_P)^{-1}$. If $R_{\bullet OH}^{tot}$ is expressed in mol s^{-1} and referred to a 22 W m^{-2} sunlight UV irradiance, $\sum_i k_{Si} [S_i]$ is in s^{-1}, and $k_{P,\bullet OH}$ is in M^{-1} s^{-1}, then the units of $(t_P^{\bullet OH})_{½}$ will be seconds of steady irradiation under 22 W m^{-2} sunlight UV. A major issue is that the outdoor sunlight intensity is not constant, and it has been shown that the integrated UV intensity over a whole sunny summer day (15 July, 45°N latitude) corresponds to 10 h irradiation at 22 W m^{-2} UV irradiance [17]. It is therefore possible to convert $(t_P^{\bullet OH})_{½}$ in units of summer sunny days (SSD, taking 15 July at 45°N latitude as reference), by dividing for 10 h = 3.6×10^4 s. The resulting half-life time for reaction with $^\bullet$OH, $(\tau_P^{\bullet OH})_{SSD}$, will therefore be expressed as follows:

$$\left(\tau_P^{\bullet OH}\right)_{SSD} = \frac{\ln 2 \cdot V \cdot \sum_i k_{Si} \cdot [S_i]}{3.6\cdot10^4 \cdot R_{\bullet OH}^{tot} \cdot k_{P,\bullet OH}} = 1.9\cdot10^{-5} \cdot \frac{V \cdot \sum_i k_{Si} \cdot [S_i]}{R_{\bullet OH}^{tot} \cdot k_{P,\bullet OH}} \qquad (25)$$

Table 1 reports the values of $(\tau_P^{\bullet OH})_{SSD}$ for a number of pesticides (the herbicides diuron, fenuron, atrazine, molinate and acetochlor, and the insecticide terbufos). The values of $k_{P,\bullet OH}$ for each

substrate are reported in Table 2 [36-40]. Note that the higher is $(\tau_P^{\bullet OH})_{SSD}$, the lower is the probability that the reaction with $^{\bullet}OH$ is an important removal pathway for the compound P.

In Table 1 it can be observed that there is both variability of $(\tau_P^{\bullet OH})_{SSD}$ for the same substrate in different water bodies, and variability among different substrates in the same water body. The degradation kinetics for the reaction with $^{\bullet}OH$ can be expected to depend on the ecosystem variables, even more than it depends on the intrinsic reactivity of the substrate. Note that in equation (25) the ecosystem-related quantities (ability to produce and consume $^{\bullet}OH$, depth of the water column) are expressed by the product $(R_{\bullet OH}^{tot})^{-1}$ V $\sum_i k_{Si}$ $[S_i]$, while the reactivity of the substrate is expressed by $k_{P,\bullet OH}$. Interestingly, as far as the ecosystem variables are concerned, an important difference can be noticed between the Lakes Avigliana Grande, Avigliana Piccolo and Candia on the one side, and the shallower water bodies (Lake Rouen, the lagoon in the Rhône delta) on the other side. It is apparent from Table 1 that the lifetimes are considerably longer for the deeper compared to the shallower systems, which suggests that the depth d of the water column could play a comparable or even a more important role than the chemical composition in the determination of the importance of the photochemical reactions. The main issue is that the intensity of radiation absorption is not linearly proportional to d, because the bottom layers of the deeper water bodies are in the dark. They do not contribute to photochemistry but constitute a reservoir of degradable compounds, which is quantified by the term V in equation (25).

2.5. Comparison with field data

The model described in the present paper was compared with the experimental data of $[^{\bullet}OH]$ measured in the top layer (1 m column depth) of Lake Greifensee, Switzerland [18]. Because the mass approach of our model does not give a direct estimate of $[^{\bullet}OH]$, the comparison was carried out on the lifetimes of the selected pesticides. In the case of the Lake Greifensee it has been measured $[^{\bullet}OH] \cong 4\times10^{-17}$ M in the first metre of the water column, under irradiation conditions corresponding to the summer solstice at noon [10]. The irradiation intensity would be around 1.4 times higher than the standard we adopted [31]. Under 22 W m^{-2} UV irradiance it would be $[^{\bullet}OH] \cong 3\times10^{-17}$ M. Under steady irradiation conditions the pseudo-first order degradation rate constant of a molecule P for reaction with $^{\bullet}OH$ would be $k_P = k_{P,\bullet OH}$ $[^{\bullet}OH]$, and the corresponding half-life time in SSD would be:

$$\left(\tau_P^{\bullet OH}\right)'_{SSD} = \frac{\ln 2}{3.6\cdot10^4 \cdot k_{P,\bullet OH}\cdot[^{\bullet}OH]} = \frac{1.9\cdot10^{-5}}{k_{P,\bullet OH}\cdot[^{\bullet}OH]} \qquad (26)$$

The half-life times calculated by equation (26) are reported in Table 3, and compared with the corresponding values derived from the model (equation 25). The input data for the model were the chemical composition of the top water layer and the depth d = 1 m. The absorption spectrum of water was unfortunately not available; it was therefore modelled by means of equation (8), based on

the reported value of NPOC (3.5 mg C L^{-1}) [10]. This is the reason of the error bars associated to the values of P_a in Table 3. The half-life times obtained from the model and from the field data are not very far, which indicates that the model can be a suitable description of surface water systems. The model lifetimes are some 30% shorter compared to the field ones, and the reasons for the difference can be the following: *(i)* it was adopted equation (8) to model the absorption spectrum of water, but this is just an approximation. Figure 1 shows that the actual spectrum could be different from the modelled one. *(ii)* The behaviour of Dissolved Organic Matter (DOM) can be different in different ecosystems, not only as far as the water absorption spectrum is concerned, but also regarding the production of $^{\bullet}OH$. Accordingly, it is possible that DOM in Lake Greifensee produces less $^{\bullet}OH$ compared to the average behaviour of Figure 4.

3. Conclusions

A model was developed to foresee the lifetime of a given compound in surface water, as far as the reaction with the hydroxyl radical is concerned. The needed inputs for the calculations are the photochemically relevant composition data (NPOC, $[HCO_3^-]$, $[CO_3^{2-}]$, $[NO_3^-]$, $[NO_2^-]$), the water column depth (e.g. the average depth of the water body) and, if available, the water absorption spectrum. As a reasonable approximation the chemical parameters and the absorption spectrum should be referred to the surface water layer, where the photochemical reactions are most significant. Indeed, in the majority of the water bodies the rate of the photochemical reactions is considerably decreased below the first meter of the water column [29].

If the absorption spectrum of water is not available it is possible to approximately estimate it, albeit with some limitations, on the basis of the NPOC value (equation 8). The modelling of the water spectrum would be useful if one aims at the assessment of the general photodegradation kinetics of a molecule as a function of water composition. In this case it could be interesting to vary the chemical parameters and the column depth over a range of reasonable values, without direct reference to a particular case.

The application of the model to some real cases showed that the lifetime of the same pesticide in different water bodies can be very variable, and the variability is comparable or even much higher than for different pesticides in the same water body. These findings suggest that as far as the reactivity with $^{\bullet}OH$ is concerned, the concepts of photolability or photostability referred to a certain molecule are not absolute ones. They are rather a function of the molecule, which contributes with its value of $k_{\bullet OH}$, and of the surrounding ecosystem that defines the values of V, $R_{\bullet OH}^{tot}$, and $\Sigma_i k_{Si} [S_i]$ (see equation 25). The model lifetimes were particularly low for the shallower water bodies (Lake Rouen, Rhône delta lagoon), which suggests that the depth of the water column can be a very important parameter.

The model lifetimes were in reasonable agreement, considering the adopted approximations, with field data from the top layer (1 m depth) of Lake Greifensee (Switzerland) [10].

Acknowledgements

Financial support by PNRA – Progetto Antartide, INCA Consortium (GLOB CHEM Working Group), and Università di Torino – Ricerca Locale is gratefully acknowledged. The work of RD in Torino was supported by MIUR – Progetto India and Compagnia di San Paolo, Torino, Italy.

References

[1] M. Bucheli-Witschel and T. Egli, FEMS – Microbiol. Rev. **25**, 69 (2001).
[2] K.M. Kuivila and B.E. Jennings, Int. J. Environ. Anal. Chem. **87**, 897 (2007).
[3] B. Druzina and M. Stegu, Int. J. Environ. Anal. Chem. **87**, 1079 (2007).
[4] M.W. Lam, K. Tantuco and S.A. Mabury, Environ. Sci. Technol. **37**, 899 (2003).
[5] S. Chiron, C. Minero and D. Vione, Environ. Sci. Technol. **41**, 3127 (2007).
[6] A.L. Boreen, W.A. Arnold and K. McNeill, Aquat. Sci. **65**, 320 (2003).
[7] S. Canonica and P.G. Tratnyek, Environ. Toxicol. Chem. **22**, 1743 (2003).
[8] S. Chiron, C. Minero and D. Vione, Environ. Sci. Technol. **40**, 5977 (2006).
[9] S. Canonica, Chimia **61**, 641 (2007).
[10] J. Hoigné, in *Aquatic Chemical Kinetics*, edited by W. Stumm (Wiley, NY, 1990), pp. 43-70.
[11] J.P. Huang and S.A. Mabury, Environ. Toxicol. Chem. **19**, 1501 (2000).
[12] J.P. Huang and S.A. Mabury, Environ. Toxicol. Chem. **19**, 2181 (2000).
[13] J.P. Huang and S.A. Mabury, Chemosphere **41**, 1775 (2000).
[14] J. Mack and J.R. Bolton, J. Photochem. Photobiol. A: Chem. **128**, 1 (1999).
[15] K. Mopper and X. Zhou, Science **250**, 661 (1990).
[16] C. Richard and S. Canonica, in *The Handbook of Environmental Chemistry Vol. 2M (Environmental Photochemistry Part II)*, edited by P. Boule, D.W. Bahnemann and P.K.J. Robertson (Springer, Berlin, Heidelberg, 2005), pp. 299-323.
[17] D. Vione, G. Falletti, V. Maurino, C. Minero, E. Pelizzetti, M. Malandrino, R. Ajassa, R.I. Olariu and C. Arsene, Environ. Sci. Technol. **40**, 3775 (2006).
[18] R.G. Zepp, J. Hoigné and H. Bader, Environ. Sci. Technol. **21**, 443 (1987).
[19] T. Brinkmann, P. Hörsch, D. Sartorius and F.H. Frimmel, Environ. Sci. Technol. 37, 3004 (2003).
[20] D.A. Skoog and J.J. Leary, *Principles of Instrumental Analysis, 4th Ed.* (Saunders College Publishing, Philadelphia, PA, 1992).
[21] D. Vione, V. Lauri, C. Minero, V. Maurino, M. Malandrino, M.E. Carlotti, R.I. Olariu and C. Arsene, Aquat. Sci., accepted.
[22] J.L. Oliveira, M. Boroski, J.C.R.Azevedo and J. Nozaki, Acta Hydrochim. Hydrobiol. **34**, 608 (2006).

[23] C. Minero, V. Lauri, G. Falletti, V. Maurino, E. Pelizzetti and D. Vione, Ann. Chim. (Rome) **97**, 1107 (2007).
[24] R. Del Vecchio and N.V. Blough, Mar. Chem. **78**, 231 (2002).
[25] N. V. Blough and R. Del Vecchio, in *Biogeochemistry of Marine Dissolved Organic Matter*, edited by D.A. Hansell and C.A. Carlson (Academic Press, Amsterdam, 2002), pp. 509-546.
[26] C. Minero, S. Chiron, G. Falletti, V. Maurino, E. Pelizzetti, R. Ajassa, M.E. Carlotti and D. Vione, Aquat. Sci. **69**, 71 (2007).
[27] L. Bracchini, A. Cozar, A.M. Dattilo, M. Falcucci, R. Gonzales, S. Loiselle and V. Hull, Chemosphere **57**, 1245 (2004).
[28] C. Minero, V. Lauri, V. Maurino, E. Pelizzetti and D. Vione, Ann. Chim. (Rome) **97**, 685 (2007).
[29] D. Vione, C. Minero, V. Maurino and E. Pelizzetti, Ann. Chim. (Rome) **97**, 699 (2007).
[30] A. Huber, G.N. Ivey, G. Wake and C.E. Oldham, J. Hydr. Eng. – ASCE **134**, 1464 (2008).
[31] R. Frank and W. Klöpffer, Chemosphere **17**, 985 (1988).
[32] S.E. Braslavsky, Pure Appl. Chem. **79**, 293 (2007).
[33] P. Warneck and C. Wurzinger, J. Phys. Chem. **92**, 6278 (1988).
[34] G.V. Buxton, C.L. Greenstock, W.P. Helman and A.B. Ross, J. Phys. Chem. Ref. Data **17**, 513 (1988).
[35] P. Westerhoff, R. Song, G. Amy and R. Minear, J. Am. Water Works Assoc. **89**, 82 (1998).
[36] F.J. Benitez, F.J. Real, J.L. Acero and C. Garcia, Wat. Res. **41**, 4073 (2007).
[37] J. De Laat, P. Maouala Makata and M. Doré, Environ. Technol. **17**, 707 (1996).
[38] A. Tauber and C. von Sonntag, Acta Hydrochim. Hydrobiol. **28**, 15 (2000).
[39] H. Shemer, C.M. Sharpless, M.S. Elovitz and K.G. Linden, Environ. Sci. Technol. **40**, 4460 (2006).
[40] P.L. Brezonik and J. Fulkerson-Brekken, Environ. Sci. Technol. 32, 3004 (1998).

Table 1. Parameters of photochemical significance in the water samples under consideration [5,17,21,26]. Note that d is the average depth of the water body, and V = 1000 S d is the volume of the water column with surface S = 1.26×10^{-3} m^2. The data in the lower section of the Table were calculated based on those of the upper one. The values of P_a and $R_{\bullet OH}$ are referred to a sunlight UV irradiance of 22 W m^{-2} (see Figure 2). The four lakes are located in Piedmont, NW Italy, the Rhône delta is in S France. SSD = summer sunny days corresponding to 15 July at 45°N latitude. Error bounds: $\mu\pm\sigma$.

	Av. Piccolo	**Candia**	**Av. Grande**	**Rouen**	**Lagoon, Rhône delta**
NPOC (mg C L^{-1})	5.1	5.4	5.0	0.63	4.5
NO_3^- (M)	1.9×10^{-5}	1.6×10^{-6}	9.6×10^{-6}	1.9×10^{-5}	5.1×10^{-5}
NO_2^- (M)	1.2×10^{-6}	1.5×10^{-7}	1.4×10^{-6}	3.7×10^{-7}	3.2×10^{-6}
HCO_3^- (M)	4.0×10^{-4}	1.1×10^{-3}	3.6×10^{-3}	2.4×10^{-5}	2.1×10^{-3}
CO_3^{2-} (M)	1.1×10^{-6}	6.1×10^{-6}	4.8×10^{-5}	2.4×10^{-9}	2.6×10^{-5}
d (m)	7.7	5.9	19.5	2.0	1.0
V (L)	9.7	7.4	24.6	2.5	1.3
P_a^{tot} (einstein s^{-1})	3.2×10^{-7}	2.5×10^{-7}	3.2×10^{-7}	1.9×10^{-7}	1.7×10^{-7}
P_a^{DOM} (einstein s^{-1})	3.2×10^{-7}	2.5×10^{-7}	3.2×10^{-7}	1.9×10^{-7}	1.7×10^{-7}
P_a^{NO3-} (einstein s^{-1})	1.1×10^{-11}	1.9×10^{-12}	1.3×10^{-11}	9.1×10^{-11}	6.9×10^{-11}
P_a^{NO2-} (einstein s^{-1})	6.3×10^{-11}	2.0×10^{-11}	2.3×10^{-10}	1.1×10^{-10}	3.6×10^{-10}
$R_{\bullet OH}^{DOM}$ (mol s^{-1})	$(9.6\pm1.3)\times10^{-11}$	$(7.5\pm1.0)\times10^{-12}$	$(9.6\pm1.3)\times10^{-12}$	$(5.7\pm0.8)\times10^{-12}$	$(5.1\pm0.7)\times10^{-12}$
$R_{\bullet OH}^{NO3-}$ (mol s^{-1})	$(4.8\pm0.2)\times10^{-13}$	$(8.2\pm0.3)\times10^{-14}$	$(5.6\pm0.2)\times10^{-13}$	$(3.9\pm0.2)\times10^{-12}$	$(3.0\pm0.1)\times10^{-12}$
$R_{\bullet OH}^{NO2-}$ (mol s^{-1})	$(7.3\pm0.2)\times10^{-12}$	$(2.3\pm0.1)\times10^{-12}$	$(2.7\pm0.1)\times10^{-11}$	$(1.3\pm0.1)\times10^{-11}$	$(4.2\pm0.1)\times10^{-11}$
$R_{\bullet OH}^{tot}$ (mol s^{-1})	$(1.7\pm0.2)\times10^{-11}$	$(9.9\pm1.1)\times10^{-12}$	$(3.7\pm0.2)\times10^{-11}$	$(2.2\pm0.2)\times10^{-11}$	$(5.0\pm0.2)\times10^{-11}$
$\Sigma_i k_{Si} [S_i]$ (s^{-1})	2.7×10^{5}	2.8×10^{5}	3.2×10^{5}	3.5×10^{4}	2.8×10^{5}
$\tau^{\bullet OH}_{Diuron}$ (SSD)	600±70	810±100	830±100	15±2	28±3
$\tau^{\bullet OH}_{Fenuron}$ (SSD)	430±50	580±70	590±70	11±1	20±2
$\tau^{\bullet OH}_{Atrazine}$ (SSD)	1000±100	1400±200	1400±200	26±3	47±6
$\tau^{\bullet OH}_{Molinate}$ (SSD)	430±50	590±70	600±70	11±1	20±2
$\tau^{\bullet OH}_{Acetochlor}$ (SSD)	400±50	540±60	550±60	10±1	19±2
$\tau^{\bullet OH}_{Terbufos}$ (SSD)	270±30	370±40	380±40	7.0±0.8	13±2

Table 2. Reaction rate constants with •OH of the selected pesticides.

Compound		**$k_{•OH}$, M^{-1} s^{-1}**	**Reference**
Diuron	Herbicide	5×10^{9}	[36]
Fenuron	Herbicide	7×10^{9}	[37]
Atrazine	Herbicide	3×10^{9}	[38]
Molinate	Herbicide	6.9×10^{9}	[39]
Acetochlor	Herbicide	7.5×10^{9}	[40]
Terbufos	Insecticide	1.1×10^{10}	[39]

Table 3. Comparison between our model, applied to the top 1 m of the Lake Greifensee (Switzerland), and the field data derived from Ref. [10]. The half-life time of the pesticides was calculated by means of equation (25) in the case of the model, and with equation (26) and the value of [$^{\bullet}$OH] (Ref. [10], corrected for a UV irradiance of 22 W m^{-2}) for the field data. The input data of equation (25) are reported in the Table, and were calculated as described in the text. The values of P_a and $R_{\bullet OH}$ are referred to a sunlight UV irradiance of 22 W m^{-2} (see Figure 2). SSD = summer sunny days corresponding to 15 July at 45°N latitude. Error bounds: $\mu \pm \sigma$.

Lake Greifensee	**Present model**	**Field data [18]**
NPOC (mg C L^{-1})	3.5	3.5
NO_3^- (M)	$1 \cdot 10^{-4}$	$1 \cdot 10^{-4}$
HCO_3^- (M)	$2 \cdot 10^{-3}$	$2 \cdot 10^{-3}$
CO_3^{2-} (M)	$1 \cdot 10^{-5}$	$1 \cdot 10^{-5}$
d (m)	1	1
V (L)	1.3	
P_a^{tot} (einstein s^{-1})	$(1.4 \pm 0.4) \cdot 10^{-7}$	
P_a^{DOM} (einstein s^{-1})	$(1.4 \pm 0.4) \cdot 10^{-7}$	
P_a^{NO3-} (einstein s^{-1})	$(1.7 \pm 0.5) \cdot 10^{-10}$	
$R_{\bullet OH}^{DOM}$ (mol s^{-1})	$(4.2 \pm 1.5) \cdot 10^{-12}$	
$R_{\bullet OH}^{NO3-}$ (mol s^{-1})	$(7.4 \pm 2.5) \cdot 10^{-12}$	
$R_{\bullet OH}^{tot}$ (mol s^{-1})	$(1.2 \pm 0.4) \cdot 10^{-11}$	
$\Sigma_i k_{Si} [S_i]$ (s^{-1})	$2 \cdot 10^{5}$	
[$^{\bullet}$OH], M		$3 \cdot 10^{-17}$
$\tau^{\bullet OH}_{Diuron}$ (SSD)	85±33	130
$\tau^{\bullet OH}_{Fenuron}$ (SSD)	61±24	90
$\tau^{\bullet OH}_{Atrazine}$ (SSD)	140±60	210
$\tau^{\bullet OH}_{Molinate}$ (SSD)	62±24	90
$\tau^{\bullet OH}_{Acetochlor}$ (SSD)	57±22	85
$\tau^{\bullet OH}_{Terbufos}$ (SSD)	39±15	60

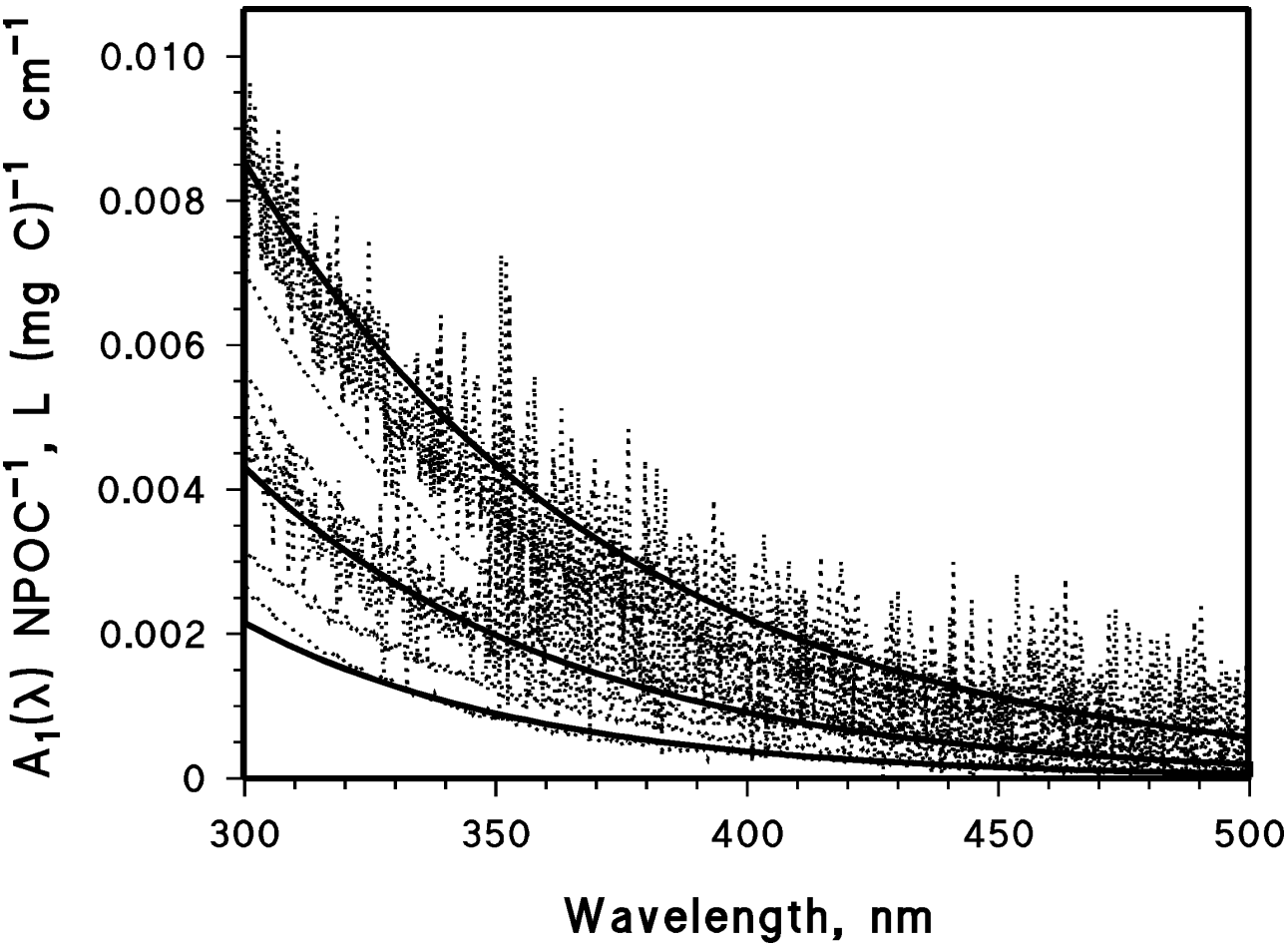

Figure 1. Absorption spectra $A_1(\lambda)$ of nine lake water samples [17,21,26]. The fitting equation (8) is also reported (bold style), together with its error bounds.

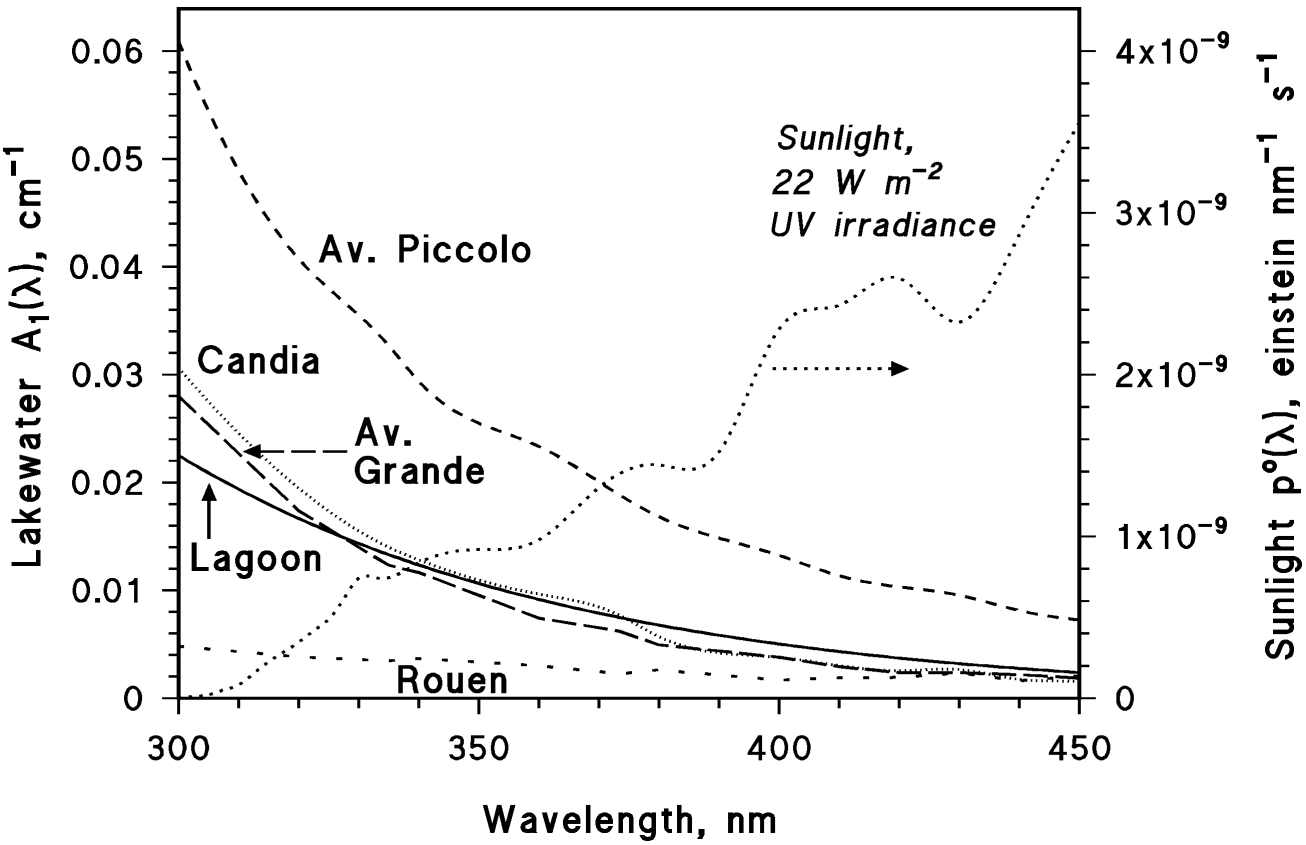

Figure 2. Absorption spectra of the water samples to which the model was applied. The lakes are all located in NW Italy, the Rhône delta lagoon is in S France [5,17,21,26]. The figure also reports the spectrum of sunlight (summer conditions, 22 W m^{-2} UV irradiance [31]).

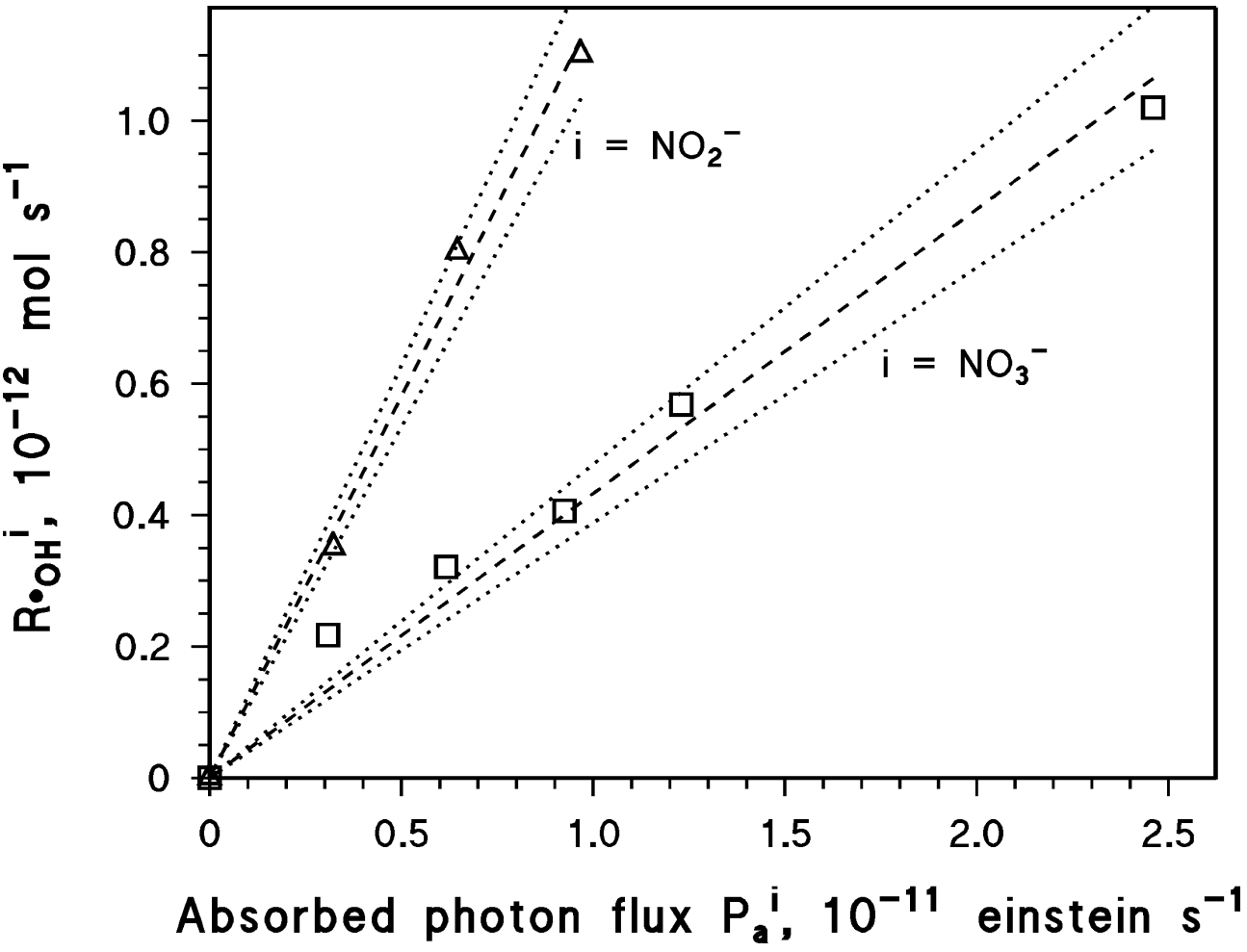

Figure 3. Initial formation rates of •OH by nitrate and nitrite ($R_{\bullet OH}^{NO3-}$, $R_{\bullet OH}^{NO2-}$) as a function of the respective absorbed photon fluxes (P_a^{NO3-}, P_a^{NO2-}), based on experimental data from Ref. [26]. UV irradiance: 22 W m^{-2}. The dashed line represents the linear regression to the experimental data, the dotted ones are the 95% confidence bounds.

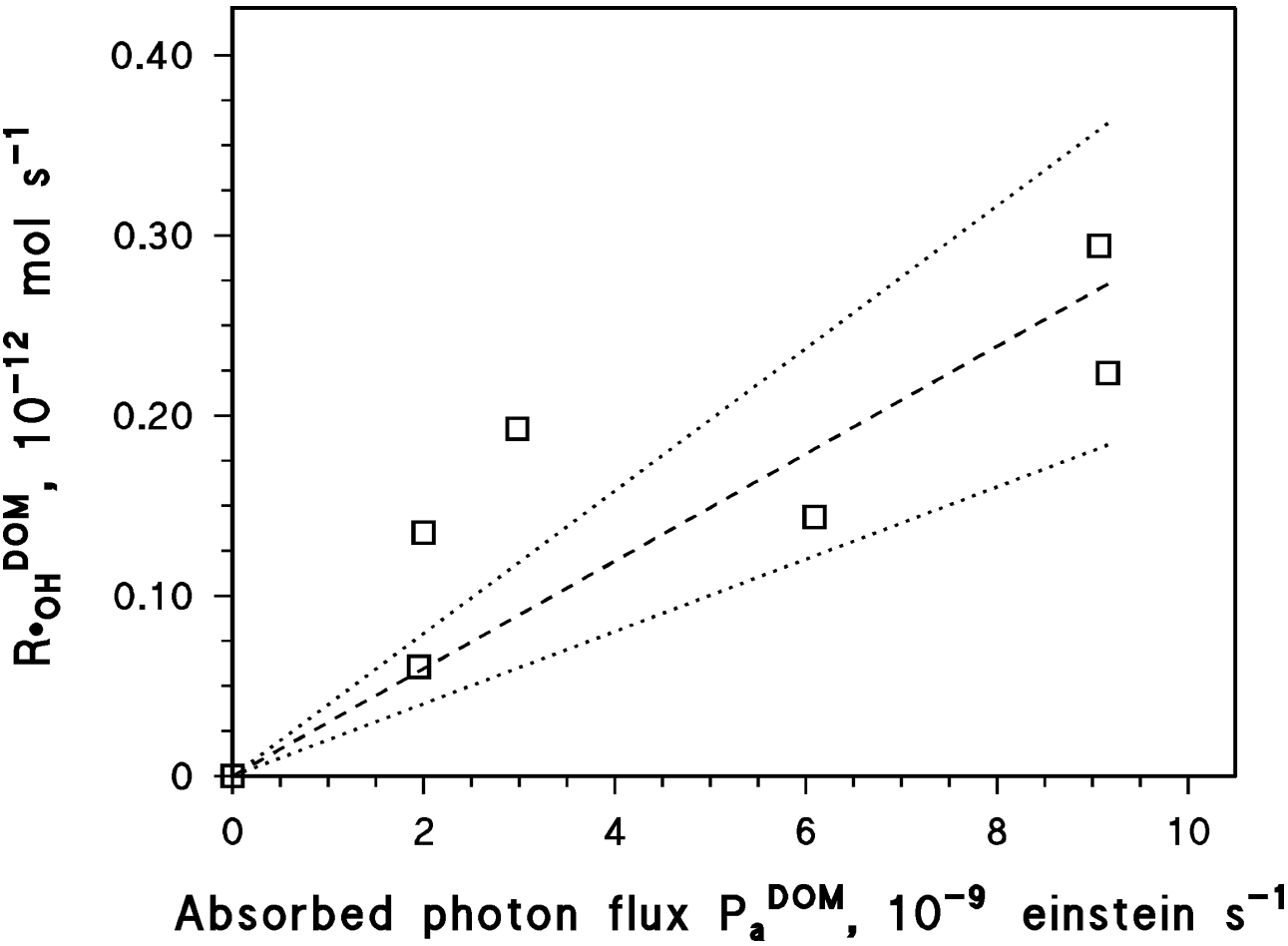

Figure 4. Initial formation rates of $^{\bullet}$OH attributable to DOM ($R_{\bullet OH}^{DOM} = R_{\bullet OH}^{tot} - R_{\bullet OH}^{NO3-} - R_{\bullet OH}^{NO2-}$) as a function of the absorbed photon flux ($P_a \approx P_a^{DOM}$), based on experimental data from Ref. [17]. UV irradiance: 22 W m^{-2}. The dashed line represents the linear regression to the experimental data, the dotted ones are the 95% confidence bounds.